

PNNL-35504

Radiation Aging of Cable Insulation Systems to Support Extension of Cable Electrical Assessment Techniques

December 2023

MK Murphy
MA Heine
M Elen
LS Fifield
L Vasilak
RN Easterling
D Rouison

DISCLAIMER

This report was prepared as an account of work sponsored by an agency of the United States Government. Neither the United States Government nor any agency thereof, nor Battelle Memorial Institute, nor any of their employees, makes **any warranty, express or implied, or assumes any legal liability or responsibility for the accuracy, completeness, or usefulness of any information, apparatus, product, or process disclosed, or represents that its use would not infringe privately owned rights.** Reference herein to any specific commercial product, process, or service by trade name, trademark, manufacturer, or otherwise does not necessarily constitute or imply its endorsement, recommendation, or favoring by the United States Government or any agency thereof, or Battelle Memorial Institute. The views and opinions of authors expressed herein do not necessarily state or reflect those of the United States Government or any agency thereof.

PACIFIC NORTHWEST NATIONAL LABORATORY
operated by
BATTELLE
for the
UNITED STATES DEPARTMENT OF ENERGY
under Contract DE-AC05-76RL01830

Radiation Aging of Cable Insulation Systems to Support Extension of Cable Electrical Assessment Techniques

December 2023

MK Murphy
MA Heine
M Elen
LS Fifield
L Vasilak
RN Easterling
D Rouison

Prepared for
the U.S. Department of Energy
under Contract DE-AC05-76RL01830

Pacific Northwest National Laboratory
Richland, Washington 99354

Acknowledgments

This work was performed at the Pacific Northwest National Laboratory Radiological Exposures & Metrology (REM) Laboratory in Richland, Washington in project NE-21-26492 “Extension of Cable Electrical Assessment Techniques to Detect and Discriminate Radiation Aging on Cable Insulation Systems” funded by the U.S. DOE Office of Nuclear Energy Gateway for Accelerated Innovation in Nuclear voucher program under the leadership of Innovation & Technology manager Christopher Lohse. The Pacific Northwest National Laboratory is operated by Battelle for the U.S. Department of Energy under Contract DE-AC05-76RL01830.

Table of Contents

| | |
|--|-----|
| Acknowledgments..... | iii |
| Table of Figures..... | v |
| Table of Tables..... | vi |
| 1.0 BACKGROUND..... | 7 |
| 2.0 INTRODUCTION..... | 8 |
| 3.0 TEST FACILITY, EQUIPMENT and MATERIALS..... | 8 |
| 3.1 Test Facility..... | 8 |
| 3.2 Equipment and Materials | 9 |
| 3.2.1 Electrical Cabling..... | 9 |
| 3.2.2 Radiochromic Film and Lithium Fluoride Dosimeters | 11 |
| 4.0 METHODS | 12 |
| 4.1 Irradiation Setup | 12 |
| 4.2 Use of Dosimeters to Dose Map the Mandrel Stack and Obtain Average Dose Rate Across its Volume..... | 14 |
| 4.2.1 Using Radiochromic Film for Initial Dose Map | 14 |
| 4.2.2 Using LiF Photofluorescent Dosimeters for Ongoing Dose Monitoring | 15 |
| 4.3 Live Video Monitoring to Ensure Irradiation Consistency..... | 16 |
| 4.4 Electrical Diagnostic Test Methods | 17 |
| 4.5 Test Schedule..... | 18 |
| 5.0 DATA RESULTS | 19 |
| 5.1 Delivered Dose to Cables | 19 |
| 5.2 POST-IRRADIATION ELECTRICAL DIAGNOSTIC TESTING..... | 22 |
| 5.2.1 LFDS Results | 22 |
| 5.2.2 PDC Results..... | 25 |
| 5.3 POST-IRRADIATION MATERIALS TESTING..... | 26 |
| 5.3.1 Tensile..... | 26 |
| 5.3.2 Indenter | 28 |
| 5.3.3 OITP..... | 29 |
| DOSE TRACEABILITY AND MEASUREMENT UNCERTAINTY | 30 |
| 6.0 30 | |
| 7.0 CONCLUSIONS..... | 32 |
| 8.0 REFERENCES..... | 33 |

Table of Figures

| | |
|--|----|
| Figure 1. Front and side views of the gamma-ray irradiator in the PNNL High Exposure Facility. Shown is the mandrel assembly on a spinning 2-rpm turntable in position for long term exposure utilizing the upper 70° port. | 9 |
| Figure 2. Okonite Okolon EPR cable. | 10 |
| Figure 3. Rockbestos Firewall III XLPE cable. | 10 |
| Figure 4. Samples of the MDV3 radiochromic film (left), and the EPSON model 10000XL flatbed scanner used to analyze the irradiated film. | 11 |
| Figure 5. TD-700 Laboratory Fluorimeter and Sunna LiF dosimeter films. | 12 |
| Figure 6. One of the 12" diameter outer mandrels loaded with cable (left). One of the layers of 12-in outer and 10" inner mandrels with first layer of short samples supported by wire mesh (middle). The same mandrels with second layer of short samples supported by bubble wrap (right). | 13 |
| Figure 7. Mandrel stack being positioned on turntable for irradiation using the 70° top port. The orange tape secures the PET buildup plate over the Sunna high dose dosimeters that monitor the dose. | 13 |
| Figure 8. Top view illustration of 12" and 10" diameter mandrels showing locations of dosimeter packets on outer and inner diameters of cables as well as at central void where short cable samples were located. | 14 |
| Figure 9. Sunna LiF film strip calibration curve used for this project. With this curve, the fsu from the ~500 films used throughout the project were converted to kGy and Mrad dose values. | 16 |
| Figure 10. Snip of check sheet used by operators to track irradiation duration, QA detectors, stack shift cycle, etc. | 17 |
| Figure 11. Rad Aging Plan for Mounted Cables on Cardboard Mandrels. (10 Mrad = 100 kGy) | 19 |
| Figure 12. Image of a sample of one of the Excel spreadsheets summarizing the Sunna dosimeter data and calculating the final doses for each of the locations within the mandrel stack and the resulting average dose rate across the mandrel stack volume. | 20 |
| Figure 13. (Left) EPR and (Right) XLPE single conductor tan delta spectroscopic responses across aging intervals. | 23 |
| Figure 14. (Left) EPR and (Right) XLPE mandrel tan delta spectroscopic responses across aging intervals. | 23 |
| Figure 15. Tan delta at 1 Hz for EPR samples in combined thermal and radiation aging group (red axis) and radiation aging group (black axis) and both 'mandrel' and 'single conductor' setups. | 24 |
| Figure 16. Tangent Delta at 100Hz for EPR aging group 1 (red axis) and EPR aging group 2 (black axis) and both 'mandrel' and 'single conductor' setups. | 24 |
| Figure 17. Tangent Delta at 1000Hz for EPR aging group 1 (red axis) and EPR aging group 2 (black axis) and both 'mandrel' and 'single conductor' setups. | 25 |

| | |
|--|----|
| Figure 18. Tan delta at 1000 Hz for EPR aging group 1 (red axis) and EPR aging group 2 (black axis) and both ‘mandrel’ and ‘single conductor’ setups. | 26 |
| Figure 19. Normalized tensile elongation-at-break of XLPE samples for the radiation only group (red) and the combined radiation thermal group (black). | 27 |
| Figure 20. Normalized tensile elongation-at-break of EPR samples for the radiation only group (red) and the combined radiation thermal group (black). | 28 |
| Figure 21. Indenter Modulus of EPR samples for the radiation only group (red) and the combined radiation thermal group (black) | 29 |
| Figure 22. OITP of XLPE for the radiation only group (red) and the combined radiation thermal group (black). | 30 |

Table of Tables

| | |
|---|----|
| Table 1: Manufacturer information for the cables provided to PNNL for radiation exposure. | 10 |
| Table 2: Levels of Thermal and Radiation Aging for Groups 1 and 2. | 18 |
| Table 3. The Main Irradiation Parameters and Resulting Air Kerma Doses for Each Cable. | 21 |
| Table 4. Additional Detail on the Dose Delivery to the Various Cable Mandrels. | 22 |
| Table 5. M&TE Used in Support of Sunna Film Dosimetry Calibration. | 31 |
| Table 6. Main Error Components Used to Calculate the Total Uncertainty in the Measured Dose Rate and Accumulated Doses. | 31 |

1.0 BACKGROUND

Nuclear power is responsible for nearly 20 percent of the electricity produced in the United States (Joskow 2006). Nuclear power plants (NPPs) depend on hundreds of miles of electrical cables within their infrastructure to provide power, instrumentation, and control functions. Safety-related cables must reliably perform not just during normal operations, but also following design basis events such as a loss of coolant accident to comply with plant safety design. Safety-related cables were originally qualified to the 40 years of initial plan operating licenses years (Gazdzinski 1996). With their average age exceeding 42 years and the continued reliance of the power grid on their contribution, most US plants have already applied for and receive license extensions to operate up to 60 years. A few subsequent license renewal applications, enabling plants to operate up to 80 years have begun to be submitted, with many more expected as plants continue to age. While generally quite stable in mild environments, the polymeric insulations of electrical cables can age and degrade due to environmental stresses present in certain plant locations including elevated temperature, moisture, and ionizing radiation. Of increasing importance with plant age are effective methods to detect and manage cable aging to maintain confidence in the ability of cables to perform safety functions if called upon to do so (IAEA 2012).

Information-rich non-destructive techniques for evaluating electrical cable condition include low-frequency dielectric spectroscopy (LFDS), time-domain dielectric spectroscopy (TDDS) and polarization depolarization current (PDC), which measures the dielectric properties of the polymer insulation materials. Commentary to these, reflectometry-based techniques can also identify the location of damage or degradation along the length of a cable. This can be very useful for isolating damaged portions of cables for repair in cables for which most of the length is not easily accessible for direct testing, such as buried cables. Reflectometry involves injection of a high-frequency electrical chirp into one end of the cable conductor. If the wave encounters an impedance change, part of the energy is reflected to the initiation point where it can be detected. Noise suppression techniques, such as processing the data in the frequency domain as with a frequency domain reflectometer (FDR) or a time domain reflectometer (TDR), allow interpretation of subtle, low-level reflected signals (Glass 2016, Glass 2017).

EPRI Report 3002010403 (EPRI 2017) documented the initial phase of research performed by EPRI and Kinectrics Inc on electrical diagnostics methods, where commonly used cross-linked polyethylene (XLPE) and ethylene propylene rubber (EPR) insulations were subjected to accelerated thermal aging using whole cable assemblies (multi-conductor cables) and single conductor test specimens. The impact of thermal aging on this cabling was periodically assessed using various mechanical, physio-chemical, and electrical testing (insulation resistance, LFDS, PDC) methods. Another EPRI Report 3002023733 (EPRI 2022) documents the results of laboratory testing that shows continued promise of the test methodology to identify varying levels of cable degradation for shielded polyvinyl chloride (PVC)-insulated low-voltage cables subjected to thermal aging. Other works (Verardi 2012, Suraci 2020a, and Suraci 2020b) determined the impact of radiation and radio-thermal aging on cable samples using physical, mechanical, and dielectric spectroscopy-based testing on both coaxial and twisted-pair XLPE insulation. Results indicated a good correlation between electrical permittivity responses measured through high-frequency dielectric spectroscopy with changes in mechanical and physicochemical responses. This study involves diagnostic testing of XLPE and EPR cables subjected to high doses of cobalt-60 (Co-60) gamma radiation following thermal aging. It is anticipated that this exercise will produce information needed to support the extension or expansion of electrical assessment techniques for NPP electrical cables.

2.0 INTRODUCTION

Radiation aging (primarily gamma radiation) of nuclear cables is primarily a concern for low voltage cables inside containment. Previous research by EPRI and Kinectrics to advance dielectric spectroscopy and related techniques focused on diagnosis of thermal effects. However, the corresponding electrical responses of cable systems to radiation aging have been relatively unexplored. To investigate the effects of radiation dose and thermal exposure on XLPE and EPR cabling test responses, several phases of controlled gamma radiation exposure were performed at Pacific Northwest National Laboratory (PNNL). This report covers the uniform irradiation and dose verification process performed at PNNL and the post-irradiation electrical diagnostic and materials testing performed by Kinectrics staff. These involved irradiation of nearly 300 total feet of 'Long' (30 foot) and 'Short' (6 and 12 inch) cable samples. Except for the 30-foot "Travel" cables, all the cables were previously exposed to various degrees of thermal aging at the Kinectrics laboratory near Toronto. At PNNL, the 12 mandrels of cabling were irradiated, at room temperature, using Co-60 gamma-rays to intervals of 10 million rads (10 Mrad) (100 kGy), with the highest dose mandrels reaching 60 Mrad (600 kGy). The post-irradiation electrical testing included LFDS and PDC, and the post-irradiation mechanical testing included tensile, indenter and oxidation-induction temperature (OITP) analysis. Correlation of the testing and exposure results will provide an understanding that will enable more accurate determination of cable condition (extent of damage). This will support the extension or expansion of electrical assessment techniques for NPP electrical cables – providing operators more information on which to base repair, mitigation, or replacement decisions.

3.0 TEST FACILITY, EQUIPMENT and MATERIALS

3.1 Test Facility

The gamma-ray irradiator used for the delivery of high radiation doses to the subject electrical cables resides within the High Exposure Facility (HEF), located at Building 318 at PNNL. The custom irradiator contains an underground shielded carousel that accommodates seven sources. It currently holds six stations to accommodate cesium-137 and Co-60 sources that vary from low- to ultra-high activity levels, resulting in a continuum of available dose rates from approximately 30 μ rad/h (300 nGy/h) to over 5 Mrad/h (50 kGy/h). The irradiator has a lower port that produces a 30° collimated beam, and an upper port that produces a 70° collimated beam. A photo of the irradiator with the stack of cable spools (hereto referred to as mandrels) staged in the optimum location in the upper port for maximum average dose rate across the mandrel volume is provided in **Figure 1**. The source used for the subject irradiations is Co-60 (#318-548), which emits 1250 keV gamma-rays and varied from 9130 to 8420 curies over the 7-month period.



Figure 1. Front and side views of the gamma-ray irradiator in the PNNL High Exposure Facility. Shown is the mandrel assembly on a spinning 2-rpm turntable in position for long term exposure utilizing the upper 70° port.

Qualified PNNL staff operated the irradiator and performed the dosimetry measurements for the duration of the study. The post-irradiation electrical diagnostic testing, which occurred nominally at every 10 Mrad (100 kGy) dose interval, was performed by qualified Kinectrics staff in a room directly adjacent to the irradiation facility.

The reasons for selecting a Co-60 source over a cesium-137 source were:

1. A Co-60 source provides a spectrum that has an average energy somewhat higher than cesium-137, which will conservatively represent the gamma spectrum that would be associated with a nuclear reactor environment.
2. This study places the focus on total dose rather than effective energy, and the specific activity associated with Co-60 provides the ultra-high dose rates required to achieve the desired total of ~60 Mrad (~600 kGy) within a reasonable period. The upper 70° port provides a larger diameter field of radiation, allowing the mandrels to be closer to the source and to minimize the irradiation time.

3.2 Equipment and Materials

3.2.1 Electrical Cabling

The electrical cables used in this research work featured EPR and XLPE insulation materials, like those commonly found in the US NPPs. Cable descriptions are provided below in **Table 1**, and photos of cut cross-sections of the cables are provided in **Figures 2 and 3**. These cables, provided in 30-ft segments, were wrapped around heavy-duty cardboard mandrels. Additional EPR and XLPE cable sets were provided in approximately 6-in and 12-in lengths for material and electrical test samples.

Table 1: Manufacturer information for the cables provided to PNNL for radiation exposure.

| Brand | Tradename | Voltage | Insulation | Jacket | No. of Conductors |
|------------|---------------------|---------|---------------------|--------|-------------------|
| Rockbestos | Firewall III (1991) | 600 V | XLPE | CSPE | 3 |
| Okonite | Okolon (1985) | 600 V | EPR/CSPE dual layer | CSPE | 3 |

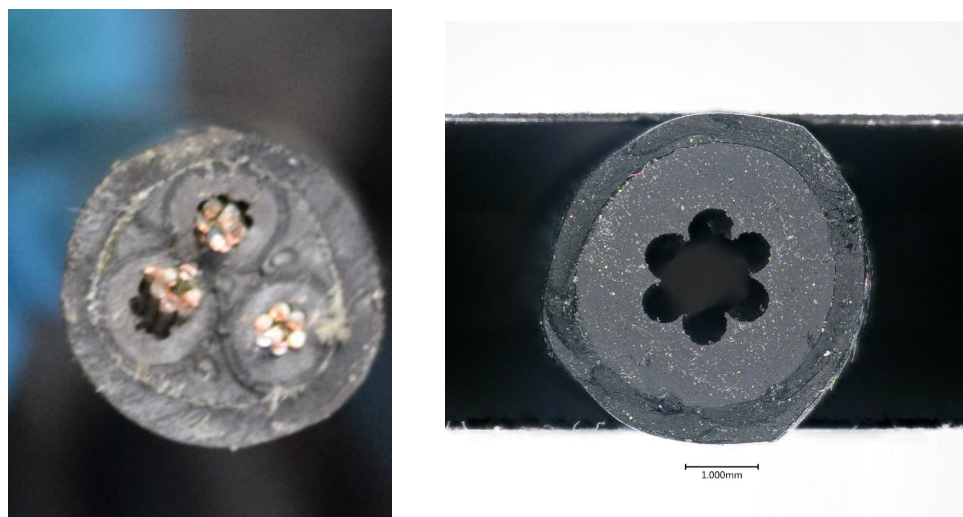


Figure 2. Okonite Okolon EPR cable.

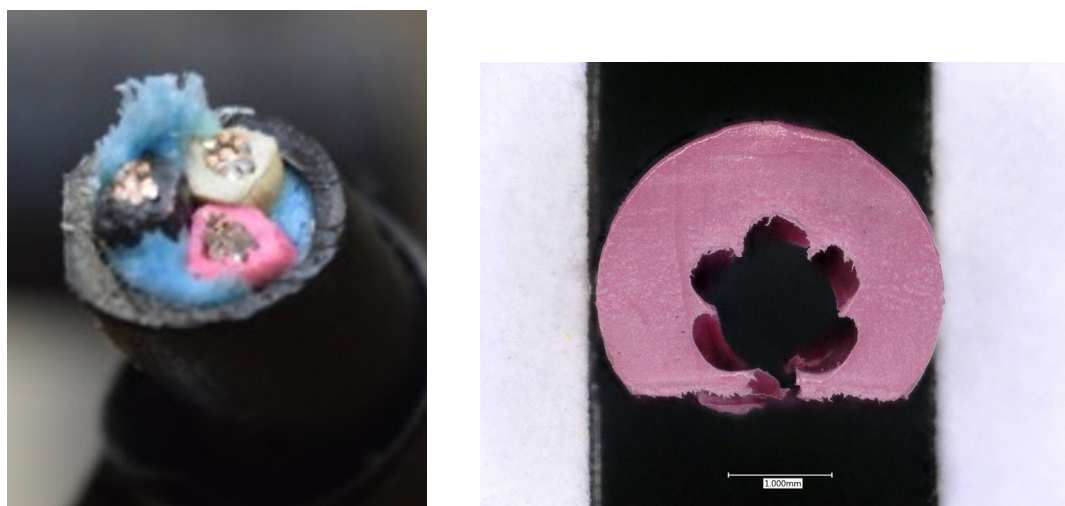


Figure 3. Rockbestos Firewall III XLPE cable.

3.2.2 Radiochromic Film and Lithium Fluoride Dosimeters

Gafchromic® Model MD-V3 radiochromic film (International Specialty Products, Wayne, NJ), cut into small formats (**Figure 4**), was used to evaluate the initial dose distribution throughout the volume of the three stacked mandrels wrapped with cable. Approximately 25 packets of the film (3 films each) were positioned throughout the Mandrel stack. The MD-V3 film was used because its sensitivity is such that the dose required for precise results only requires a few minutes of irradiation. The dose distribution can thus be mapped with an insignificant amount of dose to the mandrels.

The MD-V3 film is self-developing and can be handled in visible light. After irradiation the film undergoes a polymerization process and its color changes due to absorption bands forming in the red portion of the spectrum (absorption peaks near 636 nm). The color change is proportional to the dose received. The useful dose range of the film depends on the densitometer or spectrophotometer equipment used, but typically the range is between approximately 2 - 100 krad (2 - 100 Gy). For this study, after the film darkening was stable (MD-V3 film takes ~24 h for all dose levels) it was analyzed by measuring the absorbance or transmission of red light using an EPSON Model 10000XL flatbed scanner (EPSON America, Long Beach, CA). The mean gray scale of the scanned image was measured using ImageJ version 1.53c software. The region of interest (ROI) was defined by selecting an area of the film, and the mean gray scale was calculated using the 'Measure' function in ImageJ. This MD-V3/EPSON scanner system was calibrated using a set of the films irradiated in air to multiple National Institute of Standards and Technology (NIST)-traceable doses using a calibrated Co-60 field.

The dose values are provided in terms of Air Kerma at the location of the dosimetry, which is the standard (Kerma stands for **K**inetic **E**nergy **R**elaxed in a **M**edium). It is defined as the sum of the initial kinetic energy of all charged ionizing particles liberated by uncharged ionizing radiation in a designated mass of air. Note this is not the dose as delivered to (or absorbed by) the cables, but the dose to air at the location of the dosimetry.



Figure 4. Samples of the MDV3 radiochromic film (left), and the EPSON model 10000XL flatbed scanner used to analyze the irradiated film.

A different dosimeter had to be used to measure/monitor the dose distribution for the high dose levels associated with the long durations involved with this project – it had to be a relatively insensitive, high dose dosimeter. The Sunna LiF photofluorescent dosimeter, which has a range of approximately 0.1 - 15 Mrad (1 - 150 kGy) met this requirement. The Sunna dosimeter film consists of a polyethylene substrate with polycrystalline LiF powder mixed throughout (usually ~20% by weight). The Sunna dosimeter film used for this study was the 8-mm strip format, which is 0.25 mm thick 0.8 cm wide and 3.0 cm long, cut from a 90 m-long roll (**Figure 5**).

The irradiated dosimeters were analyzed using a model TD-700 fluorimeter (Turner Designs, Sunnyvale, CA) (**Figure 5**). The irradiated dosimeters fluoresce at ~535-nm wavelength (green) upon excitation by the 440-nm wavelength (blue) light of the fluorimeter. This green emission light is captured by the photomultiplier tube of the fluorimeter. The resulting fluorimeter signal units (fsu) are proportional to the dose received by the films; the environmental and field effects are well characterized [Murphy 2003a, Murphy 2003b, Twardowski 2011]. This Sunna/TD700 system was calibrated using a set of the films irradiated in air to multiple NIST-traceable doses using a calibrated Co-60 field.

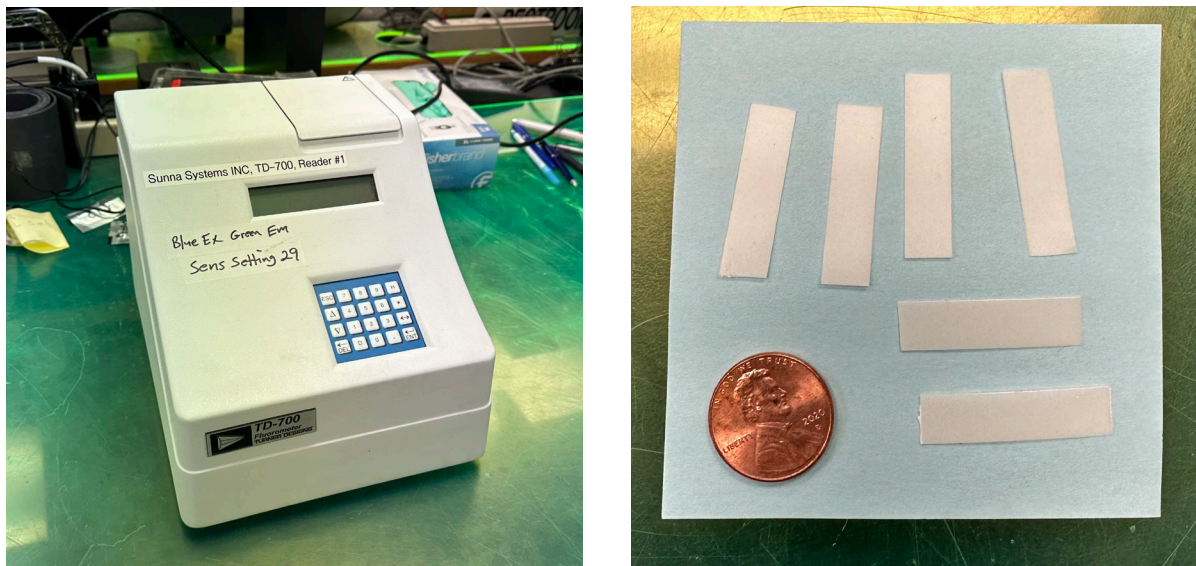


Figure 5. TD-700 Laboratory Fluorimeter and Sunna LiF dosimeter films.

4.0 METHODS

4.1 Irradiation Setup

During the initial visit of Kinectrics staff to PNNL, each of the 12, 30' cables were wrapped around the outside of 10" and 12" diameter sections cut from paperboard tubes used for pouring cylindrical concrete anchors and secured with zip ties. This tube material, constructed of 0.125" thick reinforced cardboard, was ideal because it would result in insignificant attenuation of the gamma-ray field while still providing a rigid structure. The loaded 10" mandrels were placed inside the loaded 12" mandrels, and the shorter 6" and 12" cable samples provided by Kinectrics were placed within the central voids (**Figure 6**). Given the limitations of the diameter of the

gamma-ray beam, a stack of only three mandrel sets (6 mandrels total) could be irradiated at a time, resulting in a mandrel stack of approximately 13.5" in diameter, 17" in height and 22" in maximum cross-section.

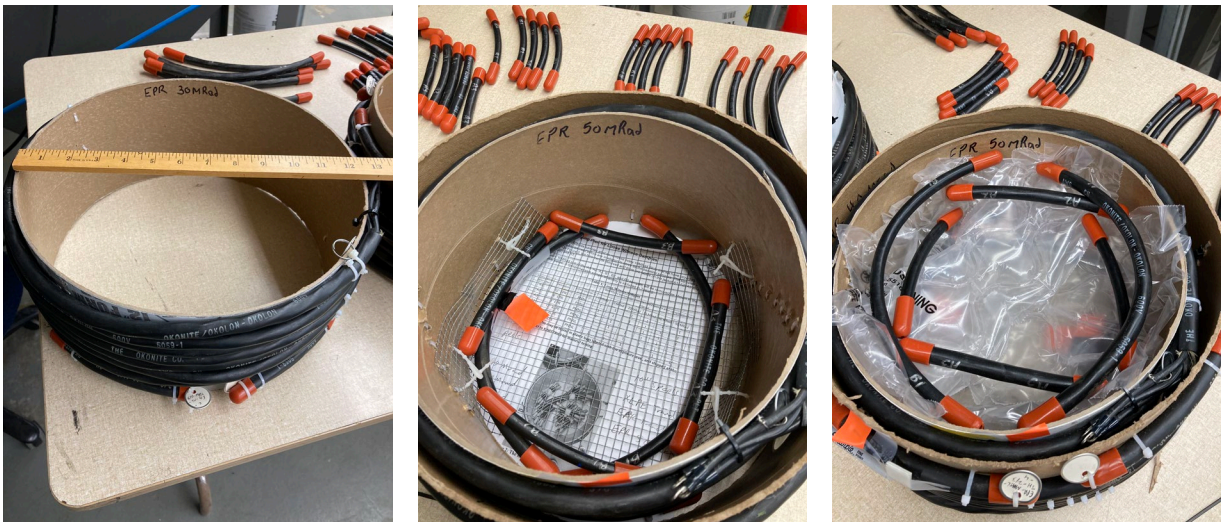


Figure 6. One of the 12" diameter outer mandrels loaded with cable (left). One of the layers of 12-in outer and 10" inner mandrels with first layer of short samples supported by wire mesh (middle). The same mandrels with second layer of short samples supported by bubble wrap (right).

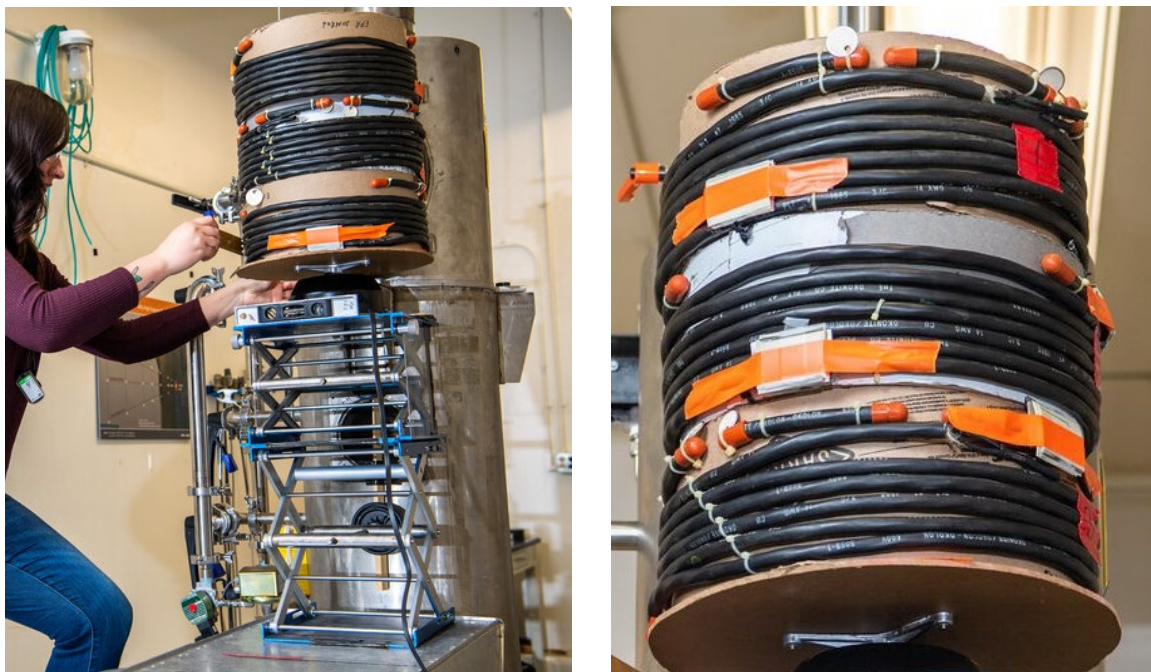


Figure 7. Mandrel stack being positioned on turntable for irradiation using the 70° top port. The orange tape secures the PET buildup plate over the Sunna high dose dosimeters that monitor the dose.

The stacked mandrel segments were centered atop a mechanical turntable that was secured in place on two lab stands (**Figure 7**). The stands and turntable were secured to prevent unintentional adjustments to the test setup over the long project. To obtain the desired total doses, the total duration within the gamma-ray field would have to be on the order of 100 days. However, the actual time to achieve the desired doses would be much longer than this because the HEF is utilized for other projects, requiring the setup to be taken down for short periods on an average of about once per week.

4.2 Use of Dosimeters to Dose Map the Mandrel Stack and Obtain Average Dose Rate Across its Volume

To maximize the delivered dose while minimizing facility and labor time required, it is necessary to characterize the dose distribution and average dose rate across the mandrel stack with the leading edges of the stack as close to the source as possible, while remaining within the beam diameter. It was determined that this ideal distance was ~44 cm, so that is the distance the central axis of the mandrel stack was placed in the upper port when the initial dose mapping was performed. Using straight edges, it was possible to visualize the beam and ensure the mandrels were completely enveloped.

4.2.1 Using Radiochromic Film for Initial Dose Map

Once the desired source-mandrel distance was identified, the dose distribution across the mandrel stack volume was mapped using the MD-V3 radiochromic film. As with the calibration film set, 10 x 10 mm squares of film within light-tight mylar pouches were used. To effectively map the uniformity of the delivered dose, 21 pouches, each containing two 5 x 5 mm films, were randomly placed in four main positions (A, B, C and D) around all three mandrels, as illustrated in **Figure 8**. These A - D position descriptors, and the associated mandrel descriptors (1, 2 and 3) were marked on the exterior of the pouches to match results with each location. Any pouches on the exterior of the mandrel were covered with an appropriate thickness of “build up” using thin PET polymer sheets. The A - D positions for the dosimeters were chosen to measure the dose delivered to the surface of the cables on the exterior of the 12” mandrels (Loc A), the interior of the cables on the 12” mandrels and the exterior of the cables on the 10” mandrels (Loc B), the interior of the cables on the 10” mandrels (Loc C), and the dose to the short samples positioned in the central voids of the mandrels (Loc D).

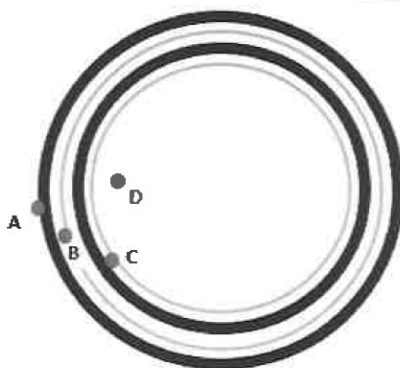


Figure 8. Top view illustration of 12” and 10” diameter mandrels showing locations of dosimeter packets on outer and inner diameters of cables as well as at central void where short cable samples were located.

For the initial dose mapping, the stacked mandrels were exposed for six 1-minute irradiations. The sequence of mandrels 1, 2 and 3 (top to bottom) was shifted between each of the six irradiations to homogenize the dose among the three mandrels within the nonuniform radiation field. To increase the dose uniformity even more, the mandrels were rotated on a motorized turntable (2 rpm) during irradiation. Following the irradiation, the films were scanned with the EPSON scanner and analyzed in the same manner as the calibration set. Using the calibration curve obtained with the calibration set of MD-V3 films, the mean gray scale values measured for the test irradiation films at each mandrel stack location were converted to the corresponding kGy and Mrad dose values. These integrated dose values were, in turn, converted to dose rates for each mandrel stack location by dividing by the corresponding irradiation durations. The arithmetic Mean of these dose rates was then used to determine the irradiation duration needed to achieve the 10 Mrad (100 kGy) intervals.

4.2.2 Using LiF Photofluorescent Dosimeters for Ongoing Dose Monitoring

Using the same naming convention and positions around the mandrels as the initial dose mapping, ~25 mylar packets, each containing three Sunna LiF dosimeters, were attached to the first set of mandrels. The 10 Mrad (100 kGy) rounds planned for the project were well within the ~15 Mrad (~150 kGy) maximum dose level for the Sunna LiF dosimeters. Because it was desired to obtain the average dose rate of the various mandrel stacks just BEFORE the desired 10 Mrad (100 kGy) was reached (to calculate the required remaining irradiation time to achieve exactly 10 Mrad (100 kGy)), the dosimeters were removed and analyzed approximately 2 days before the 10 Mrad (100 kGy) was expected to be reached. While the dosimeters were stabilized and analyzed over the following ~1.5 days, the mandrel stack irradiation continued. This dosimetry cycle was repeated for each of the 10 Mrad (100 kGy) rounds.

To obtain NIST-traceability for the associated dose rate and accumulated dose for the mandrel irradiations (in Air Kerma), the calibration curve for the Sunna dosimeters (**Figure 9**) was used to convert the fluorimeter fsu readings (from the irradiated Sunna dosimeters) to kGy and Mrad values. The associated irradiation duration was used to calculate the average dose rate value and the accumulated dose at that point in time. This information was then used to determine when the irradiation needed to stop to result in the desired 10 Mrad (100 kGy). These dosimeter results also provided the dose distribution or uniformity throughout each of the mandrel stacks involved throughout the entirety of the project. Note that throughout the duration of the project the mandrel-source distance was adjusted from the original 44 cm value to maximize the average dose rate (shortest irradiation time) while maintaining the desired dose uniformity.

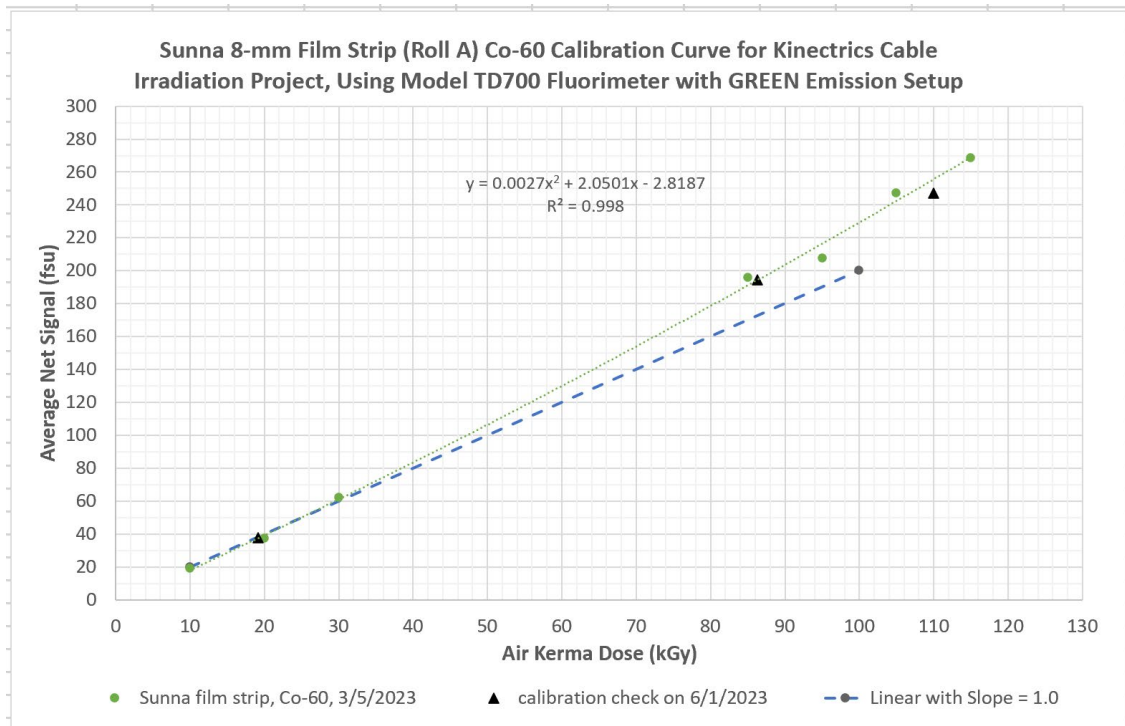


Figure 9. Sunna LiF film strip calibration curve used for this project. With this curve, the fsu from the ~500 films used throughout the project were converted to kGy and Mrad dose values.

4.3 Live Video Monitoring to Ensure Irradiation Consistency

All details of the irradiations were documented on hard copy data sheets, including date and clock times for source evolutions, mandrel stack shifting, mandrel swap outs, dosimetry swap outs, monitoring chamber readings, etc. (see example in **Figure 10**). Within the irradiation room of the HEF, the dose produces a high radiation area such that it cannot be accessed while a source is raised into the exposure column. To ensure the mandrels maintained consistent experimental conditions over the long-term irradiations (including spinning of a 2-rpm turntable and consistent reading of dose rate monitoring chamber at back of room) live video was provided with camera focused on the mandrel stack and monitoring chamber readout display on Control Panel. This live video was periodically accessed online (including nights and weekends) to ensure consistency of dose delivery, and verified and documented immediately before pausing the irradiation and immediately after resuming irradiation.

Kinectrics Cable Irradiations on Spools – Record of Durations and Dose

Facility: PNNL High Dose Gamma Facility, 70° Beam

Dose Calibration: Both A12 ionization chamber and LIF film

Cobalt-60 Source: PNNL #318-548, ~9150 Curies

* T = Top M = Middle B = Bottom of spool stack

| Run# | Date/Time | Timer Reading (min) | Spool Stack Sequence | Comments |
|------|-----------------|--------------------------------------|---|--|
| | | | Tout/Tin Mout/Min Bout/Bin | |
| 2 | 4/28/23 4:28 PM | 5760 | 1 ₂ 3 QC ~1880-1910 RAM ~25 | Resumed run after Lindsay testing at 16.6 Mrad |
| 2 | 4/29 8:15 AM | 4824 | 1 ₂ 3 QC/RAM good | stopped run to shift stack. |
| 2 | 4/29 8:24 AM | 4824 | 3 ₁ 2 QC ~1920-1990 RAM ~25 | Resumed run after stack shift. |
| 2 | 4/30 12:30 AM | 3857 | 3 ₁ 2 QC/RAM good | stopped run to shift stack. |
| 2 | 4/30 12:36 AM | 3857 | 2 ₃ 1 QC ~1740-1880 RAM ~25 | Resumed run after stack shift. |
| 2 | 4/30 4:33 PM | 2901 | 2 ₃ 1 QC/RAM good | stopped run to shift stack |
| 2 | 4/30 4:38 PM | 2901 | 1 ₂ 3 QC ~1850-1890 RAM ~25 | Resumed run after stack shift. |
| 2 | 5/1 8:38 AM | 1949 | 1 ₂ 3 QC/RAM good | stopped to shift stack |
| 2 | 5/1 8:38 AM | 1949 | 3 ₁ 2 QC ~1920-2.00 RAM ~25 | Resumed run after stack shift. |
| 2 | 5/2 12:32 AM | 995 | 3 ₁ 2 QC/RAM good | stopped run to shift stack |
| 2 | 5/2 12:40 AM | 995 | 2 ₃ 1 QC ~1760-1820 RAM ~25 | Resumed run after shift. |
| 2 | 5/2 ~4:30 PM | 43 | 2 ₃ 1 | Run stopped for equal dosimetry cycles, remove dosimetry |
| | | = 5717 min | = 95.283 hrs | → 80 19.4 Mrad total |
| 2 | 5/7 2:18 PM | 10,000 | 1 ₂ 3 QC ~1870-1910 RAM ~20-25 | Resumed run after quick dose map. Need ~20 hrs for the "20 Mrad" |
| 2 | 5/8 12:36 PM | 8663 | 1 ₂ 3 QC/RAM good | stopped run to remove "20 Mrad" witness and EPR spool. |
| | | 80 20 Mrad for witness and EPR spool | | |

Figure 10. Snip of check sheet used by operators to track irradiation duration, QA detectors, stack shift cycle, etc.

4.4 Electrical Diagnostic Test Methods

Electrical diagnostic testing was performed across two sample groups, one which was thermally and radiation aged and one that was only radiation aged. For the group that was both thermally and radiation aged, the thermal aging was performed before the radiation. A sample set was thermally aged to each of the 5 thermal intervals. The 5 sample sets were then taken to PNNL for radiation aging. The comparative levels of thermal and radiation aging between the two groups are shown in **Table 2**.

Table 2: Levels of Thermal and Radiation Aging for Groups 1 and 2.

| | XLPE Aging Group 1 | EPR Aging Group 1 | Aging Group 2 (same levels applied to XLPE and EPR) |
|-------------------|-------------------------------------|------------------------------------|---|
| Baseline | 0 h @ 130°C 0 Mrad (0 kGy) | 0 h @ 130°C 0 Mrad (0 kGy) | 0 h @ 130°C 0 Mrad (0 kGy) |
| Interval 1 | 200 h @ 130°C 10 Mrad (100 kGy) | 100 h @ 130°C 10 Mrad (100 kGy) | 0 h @ 130°C 10 Mrad (100 kGy) |
| Interval 2 | 400 h @ 130°C 20 Mrad (200 kGy) | 200 h @ 130°C 20 Mrad (200 kGy) | 0 h @ 130°C 20 Mrad (200 kGy) |
| Interval 3 | 600 h @ 130°C 30 Mrad (300 kGy) | 300 h @ 130°C 30 Mrad (300 kGy) | 0 h @ 130°C 30 Mrad (300 kGy) |
| Interval 4 | 800 h @ 130°C 40 Mrad (400 kGy) | 400 h @ 130°C 40 Mrad (400 kGy) | 0 h @ 130°C 40 Mrad (400 kGy) |
| Interval 5 | 1000 h @ 130°C 50 Mrad (500 kGy) | 500 h @ 130°C 50 Mrad (500 kGy) | 0 h @ 130°C 50 Mrad (500 kGy) |
| Interval 6 | Not tested | Not tested | 0 h @ 130°C 60 Mrad (600 kGy) |

4.5 Test Schedule

Each 10 Mrad (100 kGy) interval took approximately 14 days to complete without interruptions; however, it was common for scheduled facility maintenance or another irradiation project to interrupt the mandrel irradiations. This resulted in the ~104 days of actual irradiation time stretching out to 7 calendar months. Given that there were 12 individual cable mandrels – six sets of two, each set exposed to 10, 20, 30, 40, 50 and 60 Mrad (100, 200, 300, 400, 500, and 600 kGy) – and that only 6 mandrels could be irradiated at once, each mandrel was replaced by one of the unirradiated mandrels as it reached its preselected dose. Documentation of these mandrel swap outs is provided in Tables 3 and 4.

PNNL staff hosted Kinectrics staff at the PNNL Radiological Calibration Lab located in Building 318 to perform the electrical diagnostics tests on the gamma-irradiated cables at the scheduled intervals. The Kinectrics staff member who performed the tests completed the required PNNL training and followed all required safety protocols – all under the escort of a PNNL staff member. After the initial visit to PNNL the first week of March 2023 to perform the cable baseline measurements prior to irradiation start, the Kinectrics staff visited PNNL seven additional times (4/5, 4/27, 6/14, 8/1, 8/28, 9/27 and 10/27) and performed the electrical diagnostic measurements as per the test plan outlined in **Figure 11**.

TEST MATRIX ⊕ LFDS+PDC ○ TDR △ FDR ✕ Remove from Gamma Exposure

| Sample ID | Target Irradiation Amount | 0MRad | 10MRad | 20MRad | 30MRad | 40MRad | 50MRad |
|------------|---------------------------|-------|--------|--------|--------|--------|--------|
| EPR-TH-I1 | 10MRad | ⊕○△ | ⊕○△✕ | | | | |
| EPR-TH-I2 | 20MRad | ⊕○△ | | ⊕○△✕ | | | |
| EPR-TH-I3 | 30MRad | ⊕○△ | | | ⊕○△✕ | | |
| EPR-TH-I4 | 40MRad | ⊕○△ | | | | ⊕○△✕ | |
| EPR-TH-I5 | 50MRad | ⊕○△ | | | | | ⊕○△✕ |
| XLPE-TH-I1 | 10MRad | ⊕○△ | ⊕○△✕ | | | | |
| XLPE-TH-I2 | 20MRad | ⊕○△ | | ⊕○△✕ | | | |
| XLPE-TH-I3 | 30MRad | ⊕○△ | | | ⊕○△✕ | | |
| XLPE-TH-I4 | 40MRad | ⊕○△ | | | | ⊕○△✕ | |
| XLPE-TH-I5 | 50MRad | ⊕○△ | | | | | ⊕○△✕ |
| XLPE-RAD* | 50MRad | ⊕○△ | ⊕○△ | ⊕○△ | ⊕○△ | ⊕○△ | ⊕○△✕ |
| EPR-RAD* | 50MRad | ⊕○△ | ⊕○△ | ⊕○△ | ⊕○△ | ⊕○△ | ⊕○△✕ |

Figure 11. Rad Aging Plan for Mounted Cables on Cardboard Mandrels. (10 Mrad = 100 kGy)

5.0 DATA RESULTS

5.1 Delivered Dose to Cables

The results of the numerous dose rate measurements made throughout the duration of the project using the Sunna LiF dosimeters within the mandrel stacks were calculated and summarized using a customized Excel spreadsheet. **Figure 12** shows this spreadsheet for one of the 7 rounds during the project. **Table 3** provides the main irradiation parameters and resulting Air Kerma doses. In addition to the doses associated with mandrel stack locations A - D, estimated dose values are also provided for the center of each cable. **Table 4** provides additional detail on the dose delivery to the various cable mandrels. Note that, although the total doses delivered at the dosimetry locations reached ~70 Mrad (~700 kGy) over the duration of project, the highest dose to cables was ~60 Mrad (~600 kGy). Doses in 10 Mrad (100 kGy) intervals were delivered to 12 mandrels over ~104 days of irradiation (a total period of 7 months due to pauses), with the highest dosed mandrels (the “Travel” mandrels) receiving ~60 Mrad (~600 kGy). For the seven 10 Mrad (100 kGy) rounds, the standard deviation of the dose across the entire volume of the mandrel stack (as measured by the LiF dosimetry) varied from approximately 2.0 to 4.6% (considered to be ~68% confidence level). The total uncertainty associated with the measured dose values (i.e., the accuracy relative to the NIST standard) was calculated to be 6.6% at the 95% confidence level.

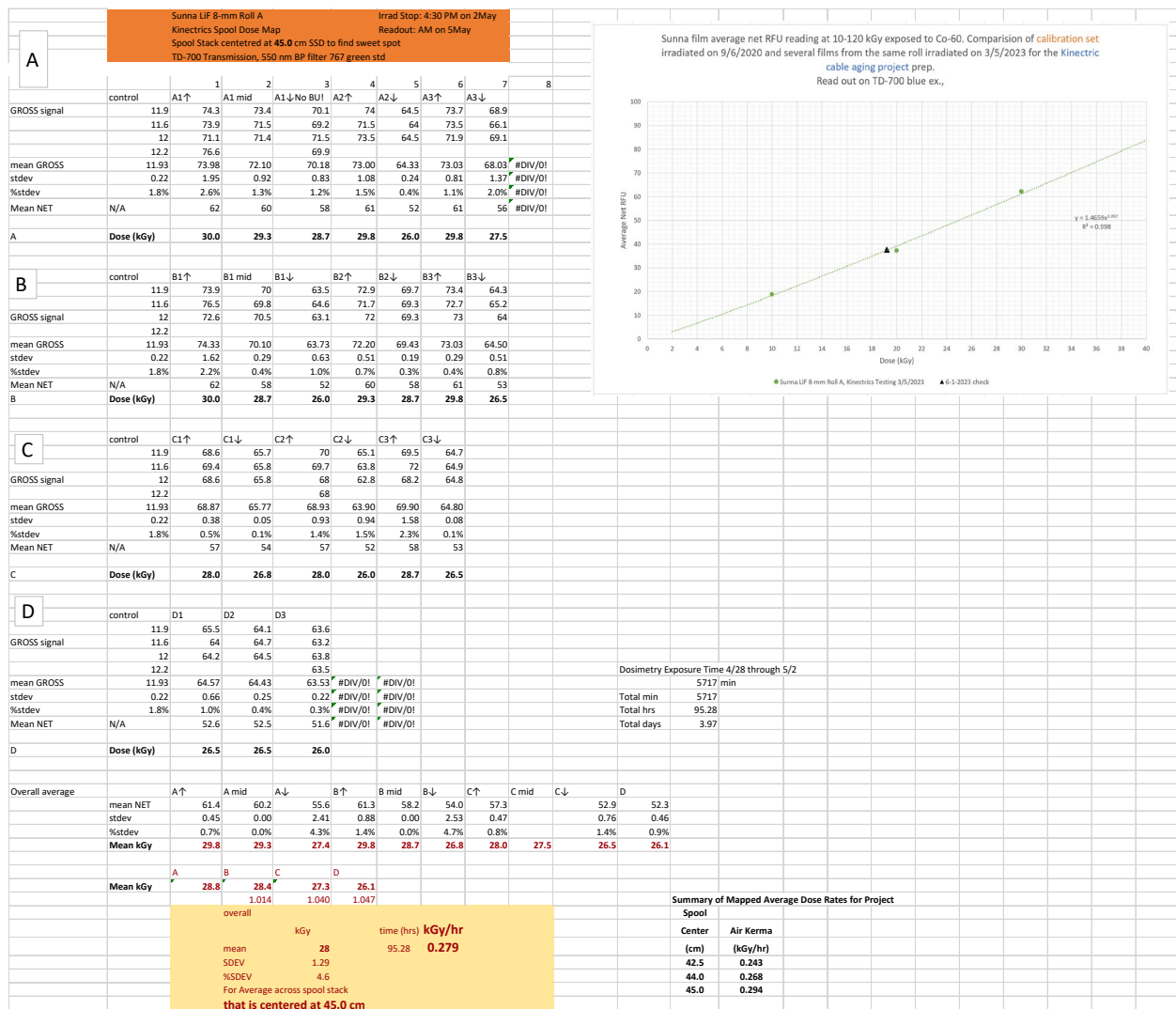


Table 3. The Main Irradiation Parameters and Resulting Air Kerma Doses for Each Cable.

| 10 Mrad Interval # | Description of Cables* On Spools During each Interval | | Spool Distance from source (cm) | Irradiation Start | Irradiation Stop | Irradiation Duration (hrs) | Measured† Average Dose Rate Across Spools (krad/hr) | Delivered Dose (Mrad)* | | | |
|--|--|-------------------------------------|---------------------------------|-------------------|------------------|----------------------------|--|------------------------|-----------------|-----------------|----------------|
| | 12" | 10" | | | | | | Average A,B,C,D | 12" Spool Cable | 10" Spool Cable | Short# Samples |
| 1 | EPR 20 EPR 30 EPR 40 | XLPE Travel EPR Travel EPR 50 | 42.5 | 3/15/2023 | 4/4/2023 | 304.3 | 0.268 | 8.15 | 8.34 | 8.13 | 7.83 |
| 1 | EPR 20 EPR 30 EPR 40 | XLPE Travel EPR Travel EPR 50 | 42.5 | 4/8/2023 | 4/10/2023 | 47.9 | 0.268 | 1.28 | 1.31 | 1.28 | 1.23 |
| 1 | | | | | | | cumulative | | 9.66 | 9.41 | 9.07 |
| 2 | EPR 20 EPR 30 EPR 40 | XLPE Travel EPR Travel EPR 50 | 45.0 | 4/12/2023 | 4/26/2023 | 305.1 | 0.247 | 7.55 | 7.73 | 7.53 | 7.25 |
| | | | | | | | cumulative | | 17.4 | 16.9 | 16.3 |
| 2 | EPR 20 EPR 30 EPR 40 | XLPE Travel EPR Travel EPR 50 | 45.0 | 4/28/2023 | 5/8/2023 | 117.6 | 0.279 | 3.28 | 3.36 | 3.27 | 3.15 |
| | | | | | | | cumulative | | 20.7 | 20.2 | 19.5 |
| 3 | XLPE 50 EPR 30 EPR 40 | XLPE Travel EPR Travel EPR 50 | 45.0 | 5/8/2023 | 6/11/2023 | 409.2 | 0.286 | 11.7 | 12.0 | 11.7 | 11.2 |
| | | | | | | | cumulative | | 32.7 | 31.9 | 32.2 |
| 4 | XLPE 50 XLPE 40 EPR 40 | XLPE Travel EPR Travel EPR 50 | 45.0 | 6/15/2023 | 7/29/2023 | 359.3 | 0.275 | 9.9 | 10.13 | 9.88 | 9.51 |
| | | | | | | | cumulative | | 42.8 | 41.8 | 42.1 |
| 5 | XLPE 50 XLPE 40 XLPE 30 | XLPE Travel EPR Travel EPR 50 | 44.0 | 8/1/2023 | 8/24/2023 | 349.6 | 0.287 | 10.0 | 10.3 | 10.0 | 9.65 |
| | | | | | | | cumulative | | 53.1 | 51.8 | 51.6 |
| 6 | XLPE 50 XLPE 40 XLPE 30 | XLPE Travel EPR Travel XLPE20 | 44.0 | 9/2/2023 | 9/24/2023 | 358.6 | 0.258 | 9.2 | 9.47 | 9.23 | 8.89 |
| | | | | | | | cumulative | | 62.6 | 61.0 | 58.8 |
| 7 | XLPE 50 XLPE 40 XLPE 30 | XLPE 10 EPR 10 XLPE 20 | 44.0 | 9/29/2023 | 10/20/2023 | 347.7 | 0.288 | 10.0 | 10.2 | 10.0 | 9.62 |
| | | | | | | cumulative | XLPE 10 and EPR 10 = 10.0 XLPE 20 = 21.6 XLPE 30 = 31.4 XLPE 40 = 40.9 XLPE 50 = 51.1 | | | | |
| * Spools in red font were removed/completed at the end of the round, and resulting dose values are also listed in red. Spools in blue font were added in that round. | | | | | | | | | | | |
| † Dose is in terms of Air Kerma. Average of all measurement points, as well as dose to center of cables. | | | | | | | | | | | |
| # At the end of each "10Mrad" interval, additional dose was added to the Short cable samples to bring dose closer to long cables. | | | | | | | | | | | |

Table 4. Additional Detail on the Dose Delivery to the Various Cable Mandrels.

| Kinectrics Cable Spool Irradiations Summary | | | | | | | | | | | | | | |
|--|----------|------------------|----------------|----------------|---------------------|---------------------------------|------|------|------|----------------------|--------------------------------|-------------------------|------|-------|
| Start Date | End Date | 10 Mrad Interval | Measured | Irradiation | Average Dose (Mrad) | Average Mrad at Spool Locations | | | | Added Mrad to Shorts | Spool Removed After this round | Mrad to Center of Cable | | |
| | | | Average kGy/hr | | | A | B | C | D | | | 12" | 10" | Short |
| | | | | Duration (hrs) | | | | | | | | | | |
| 3/15/23 | 4/4/23 | 1 | 0.268 | 304.3 | 8.15 | 8.4 | 8.3 | 8.0 | 7.8 | 0.0 | None | 8.34 | 8.13 | 7.83 |
| Travel tests 4/5 | | | cumulative | | 8.15 | 8.4 | 8.3 | 8.0 | 7.8 | 0.0 | None | 8.34 | 8.13 | 7.83 |
| Added dose 4/8 to 4/10 | | | | 47.9 | 1.28 | 1.33 | 1.30 | 1.26 | 1.23 | 0.0 | None | 1.31 | 1.28 | 1.23 |
| | | | cumulative | | 9.43 | 9.8 | 9.6 | 9.3 | 9.1 | 1.6 | None | 9.66 | 9.41 | 10.67 |
| 1.6 Mrad added to 10 Mrad Witness | | | | | | | | | | | | | | |
| 4/12/23 | 4/26/23 | 2 | 0.247 | 305.1 | 7.55 | 7.8 | 7.6 | 7.4 | 7.3 | 0.0 | None | 7.73 | 7.53 | 7.25 |
| Travel tests 4/27 | | | cumulative | | | 17.6 | 17.2 | 16.7 | 16.3 | 0.0 | None | 17.4 | 16.9 | 16.3 |
| 4/28/23 | 5/8/23 | 2 | 0.279 | 117.57 | 3.28 | 3.39 | 3.32 | 3.22 | 3.15 | 0.0 | None | 3.36 | 3.27 | 3.15 |
| No Travel tests | | | cumulative | | | 21.0 | 20.5 | 19.9 | 19.5 | 0.0 | EPR 20Mrad ~5/8 | 20.7 | 20.2 | 19.5 |
| Sunna meas indicate 0.294 kGy/h, but determined the TD700 was over-responding by 5%...so correctd to 0.279 kGy/h | | | | | | | | | | | | | | |
| 5/8/23 | 6/11/23 | 3 | 0.286 | 409.17 | 11.7 | 12.1 | 11.9 | 11.5 | 11.2 | 0.0 | None | 12.0 | 11.7 | 11.2 |
| Travel tests 6/14 | | | cumulative | | | 33.0 | 32.4 | 31.4 | 30.7 | 1.5 | EPR 30Mrad ~6/11 | 32.7 | 31.9 | 32.2 |
| 6/15/23 | 7/29/23 | 4 | 0.275 | 359.3 | 9.9 | 10.2 | 10.0 | 9.7 | 9.5 | 0.0 | | 10.13 | 9.88 | 9.51 |
| Travel tests 8/1 | | | cumulative | | | 43.3 | 42.4 | 41.1 | 40.2 | 1.9 | EPR 40Mrad ~7/29 | 42.8 | 41.8 | 42.1 |
| 8/1/23 | 8/24/23 | 5 | 0.287 | 349.6 | 10.0 | 10.4 | 10.2 | 9.9 | 9.7 | 0.0 | | 10.3 | 10.0 | 9.65 |
| 50 Mrad witness 8/25 to 8/28 | | | cumulative | | | 53.7 | 52.6 | 51.0 | 49.9 | 1.7 | EPR 50Mrad ~8/24 | 53.1 | 51.8 | 51.6 |
| Travel tests 8/28 | | | | | | | | | | | | | | |
| 9/2/23 | 9/24/23 | 6 | 0.258 | 358.6 | 9.2 | 9.6 | 9.4 | 9.1 | 8.9 | 0.0 | | 9.47 | 9.23 | 8.89 |
| | | | cumulative | | | 63.2 | 62.0 | 60.1 | 58.8 | 0.0 | Both "Travel" | 62.6 | 61.0 | 58.8 |
| Travel tests 9/27 | | | | | | | | | | | | | | |
| 9/29/23 | 10/20/23 | 7 | 0.288 | 347.7 | 10.0 | 10.4 | 10.1 | 9.8 | 9.6 | 0.0 | XLPE 10 XLPE 20 | 10.2 | 10.0 | 9.62 |
| Travel tests 10/27 | | | cumulative | | | 73.6 | 72.1 | 69.9 | 68.4 | 0.0 | XLPE 30 XLPE 40 | 72.8 | 71.0 | 68.4 |
| | | | | | | | | | | | XLPE 50 EPR 10 | | | |

5.2 POST-IRRADIATION ELECTRICAL DIAGNOSTIC TESTING

5.2.1 LFDS Results

Low-frequency dielectric spectroscopy response, in the form of the complex capacitance components C' and C'' and the associated tangent delta ($\tan \delta$) was captured from 1 mHz to 1 kHz on all cable samples. Samples were tested in two different electrical setups. One setup consisted of the 30' multiconductor (3-conductor unshielded) cable wrapped around a cardboard mandrel (named 'mandrel' samples). The second setup consisted of only a 12" single conductor (named 'single conductor' samples). Example of 'single conductor' $\tan \delta$ spectroscopic responses are shown in **Figures 13 and 14** and include the response from each consecutive aging interval.

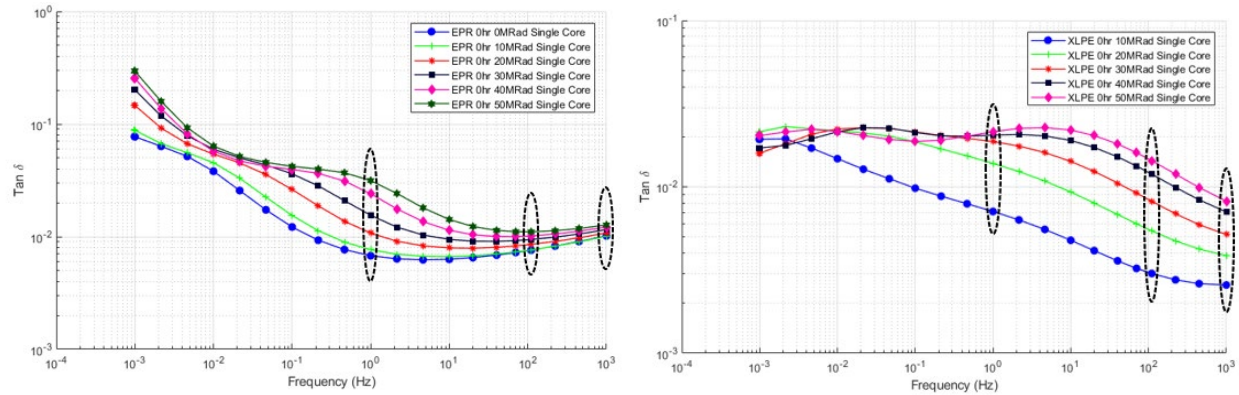


Figure 13. (Left) EPR and (Right) XLPE single conductor tan delta spectroscopic responses across aging intervals.

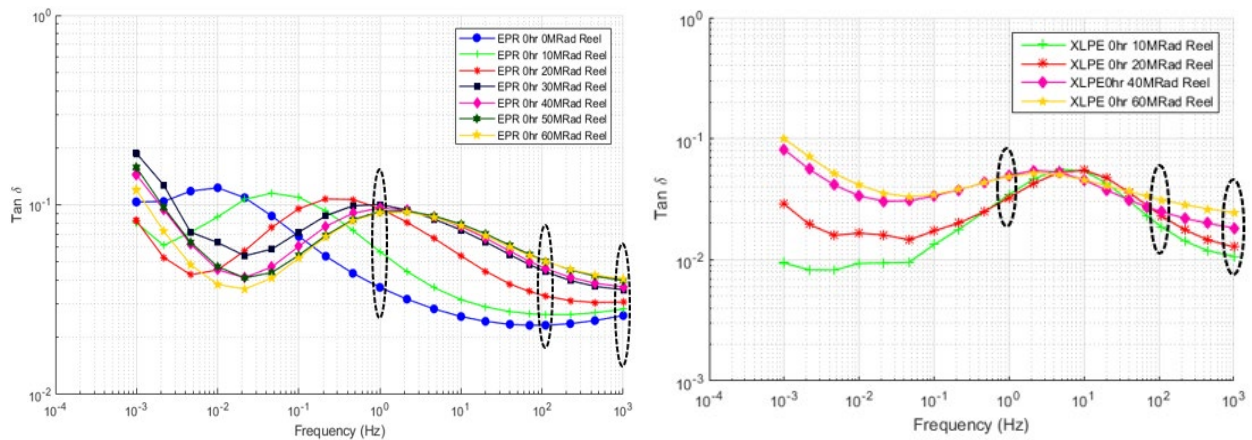


Figure 14. (Left) EPR and (Right) XLPE mandrel tan delta spectroscopic responses across aging intervals.

Spectra were noted to have different shapes across the sample groups. Discrete frequencies of 1 Hz, 100 Hz, and 1000 Hz were selected from the tan delta spectra as preliminary metrics because they showed the clearest trends across most sample groups (**Figure 15**, **Figure 16**, **Figure 17**). An increasing trend in tan delta at 1 Hz is observed for both EPR single conductor aging groups; however, the increase is larger in the radiation and thermal aged group compared to the radiation-only group (**Figure 15**). The radiation and thermal aged EPR mandrel did not show a consistent trend at 1Hz; however, in the radiation aged EPR mandrel there is an upward trend. At 100 Hz and 1000 Hz the tangent delta was observed to increase for both ‘mandrel’ and ‘single conductor’ EPR samples and both aging groups. Although the ‘single conductor’ samples showed an increase in tan delta with each subsequent aging interval at all frequencies in the range measured of 1 mHz to 1k Hz, the ‘mandrel’ sample responses were more complex. The changes in the ‘mandrel’ sample spectra are likely due to the composite system of insulation, layering, filler, and jacketing. These materials composing the overall cable system have independent responses when they undergo radiation and thermal changes and are likely the cause of the complex spectra observed (**Figure 14**). The assessment metrics presented here are the result of the preliminary analysis of the results. Additional condition indicators, especially for the more complex responses observed with the cable mandrels, will require more in-depth analysis of the data.

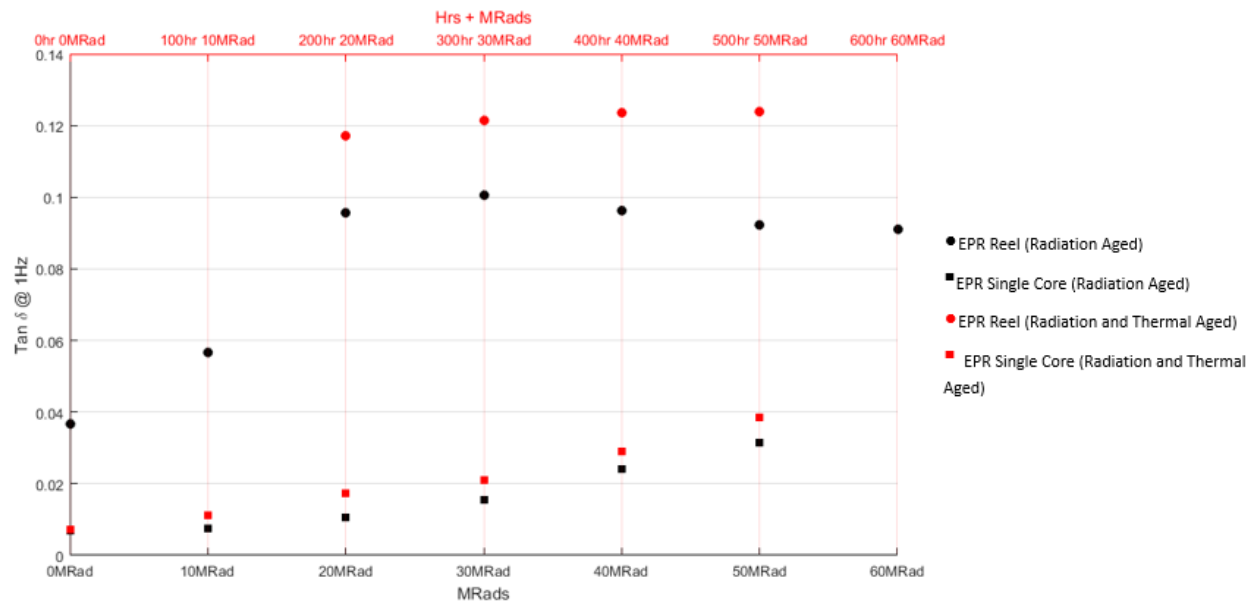


Figure 15. Tan delta at 1 Hz for EPR samples in combined thermal and radiation aging group (red axis) and radiation aging group (black axis) and both ‘mandrel’ and ‘single conductor’ setups.

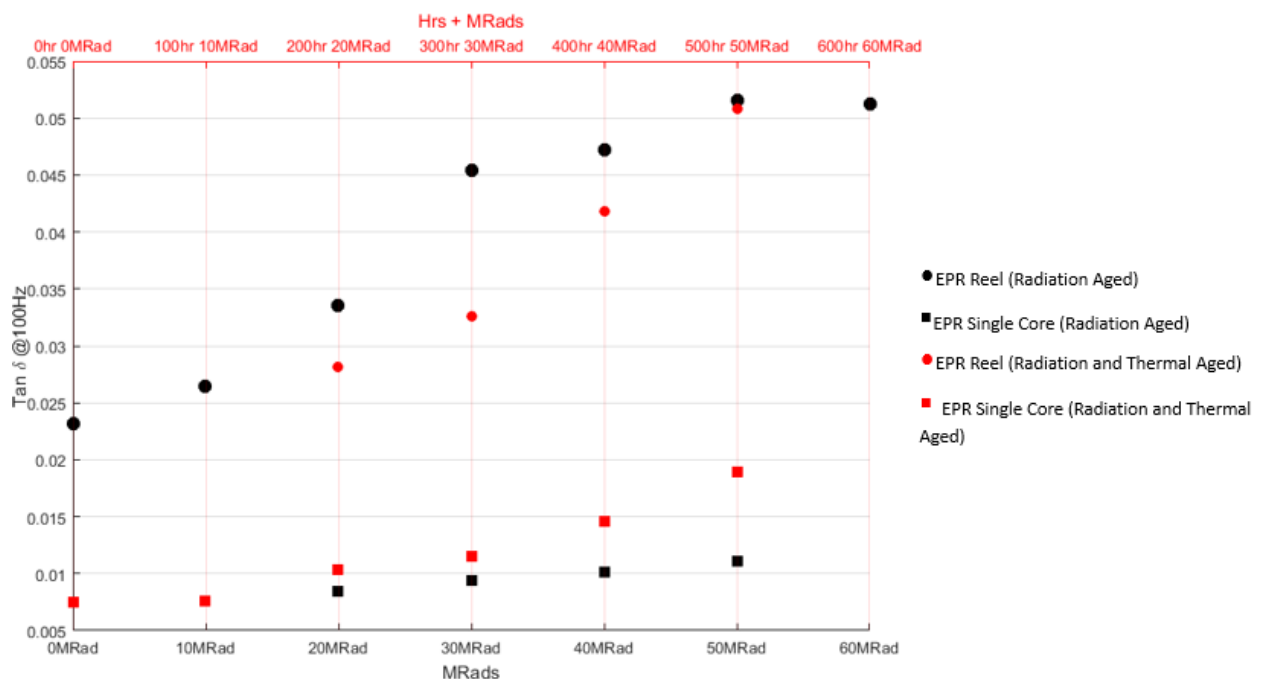


Figure 16. Tangent Delta at 100Hz for EPR aging group 1 (red axis) and EPR aging group 2 (black axis) and both ‘mandrel’ and ‘single conductor’ setups.

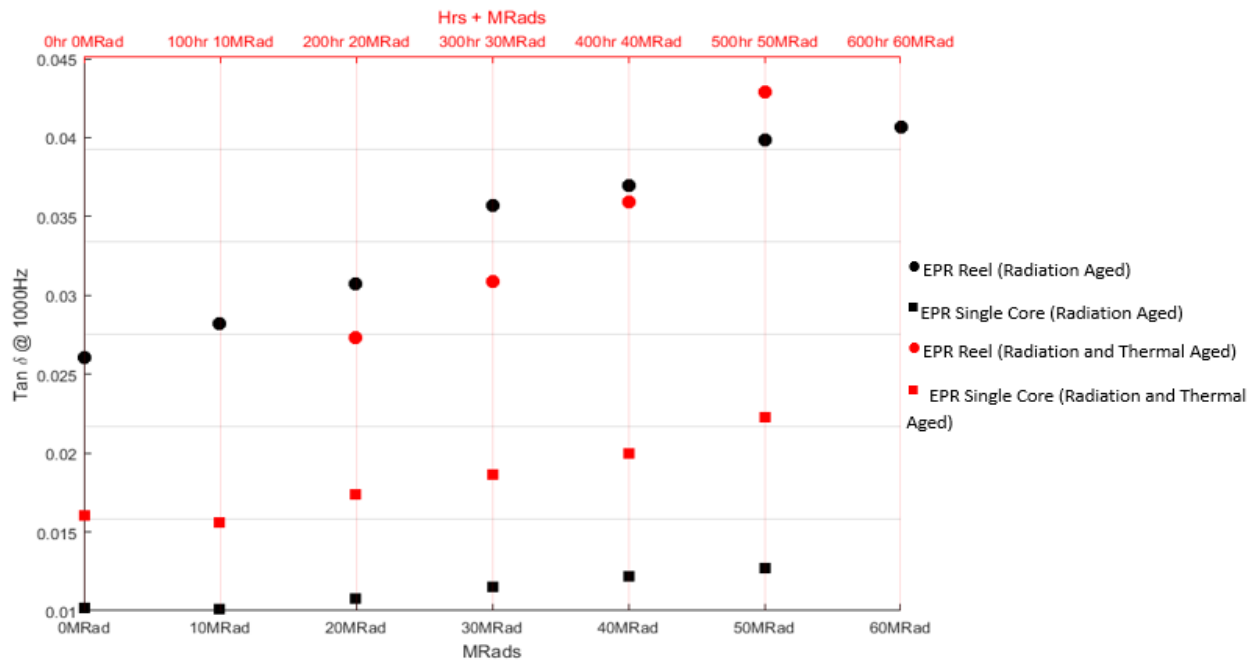


Figure 17. Tangent Delta at 1000Hz for EPR aging group 1 (red axis) and EPR aging group 2 (black axis) and both 'mandrel' and 'single conductor' setups.

5.2.2 PDC Results

Polarization and depolarization currents (PDC) were measured on all samples for a duration of 1000 s each. PDC correlations at 60 s are plotted for EPR 'single conductors' (thermal/radiation aged and radiation aged) in **Figure 18**. Different trends are noted in the responses. For single conductors exposed to both thermal and radiation aging, the polarization depolarization ratio increases along the $y = x$ line. For single conductors exposed to only radiation aging, the polarization depolarization current ratio increases away from the $y = x$ line due to increased polarization current. It was noted that PDC results for the mandrels produced a more complex response. Other metrics will require more in-depth analysis.

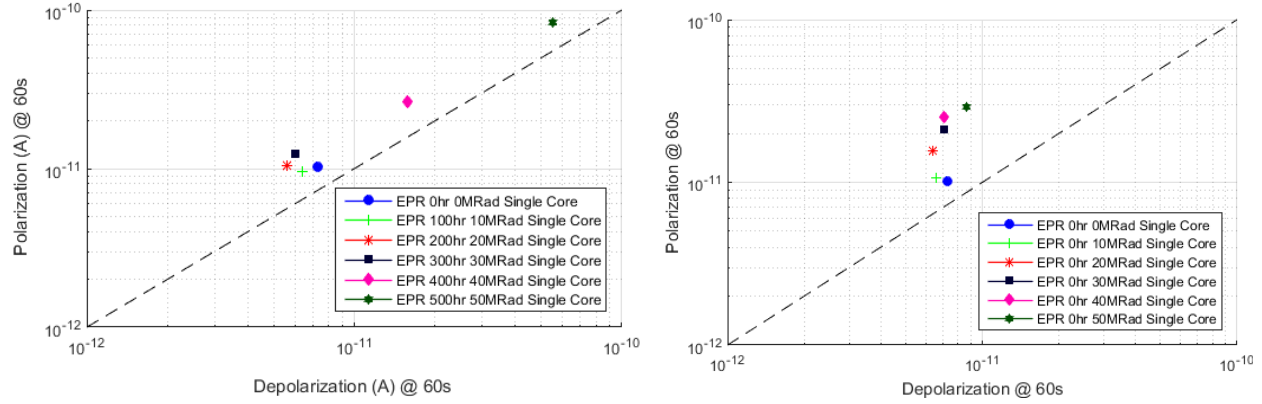


Figure 18. Tan delta at 1000 Hz for EPR aging group 1 (red axis) and EPR aging group 2 (black axis) and both 'mandrel' and 'single conductor' setups.

5.3 POST-IRRADIATION MATERIALS TESTING

5.3.1 Tensile

Tensile testing of the insulation material associated with the individual conductors was performed by Kinectrics staff to determine sample condition and gain information about sample mechanical properties in relation to the environmental aging they experienced. Although both aging regimes (thermal + rad and rad only) created a decrease in elongation-at-break (EaB) values at each subsequent aging interval, the combined thermal and radiation created a stronger decrease for both XLPE and EPR samples (**Figures 19 and Figure 20**).

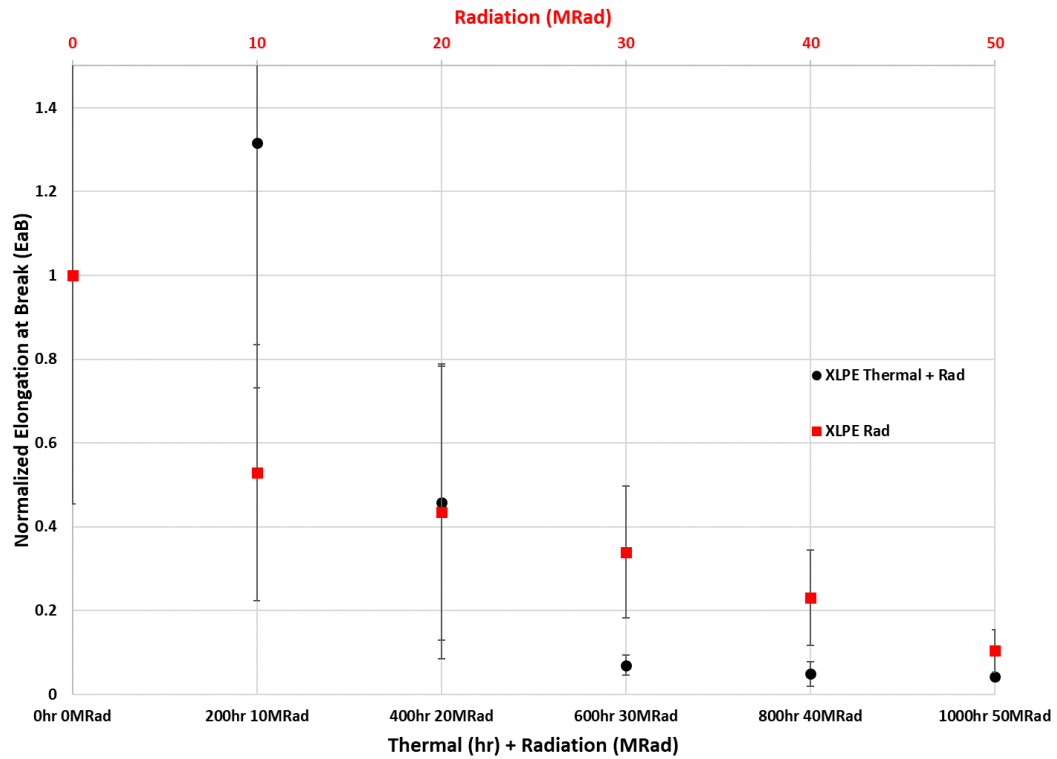


Figure 19. Normalized tensile elongation-at-break of XLPE samples for the radiation only group (red) and the combined radiation thermal group (black).

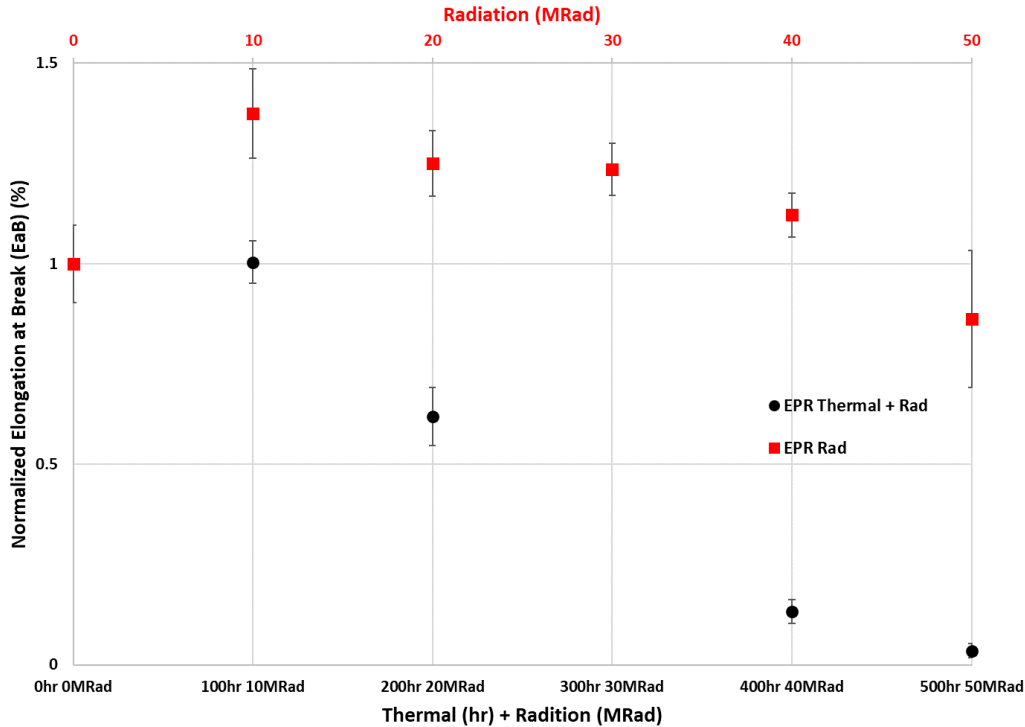


Figure 20. Normalized tensile elongation-at-break of EPR samples for the radiation only group (red) and the combined radiation thermal group (black).

5.3.2 Indenter

Indenter testing of EPR insulation samples was performed by Kinectrics staff. In this test the specimen is secured with the head clamp of the instrument and the specimen surface compressed by the indenter tip at a constant speed of 5.08 mm/min. The load, in Newtons, is recorded as a function of displacement up to a maximum of 5 N, at which point the tip is retracted to avoid damaging the specimen. The indenter modulus (IM) corresponds to the slope of the resulting curve in the 1.5 N to 3.5 N range. The IM can be compared to published data for known materials to determine if the material has experienced any degradation as a result of aging. The indenter results in **Figure 21** show that radiation aging did not create a trend in insulation hardness, whereas an increasing trend is clear for samples subjected to progressive thermal aging.

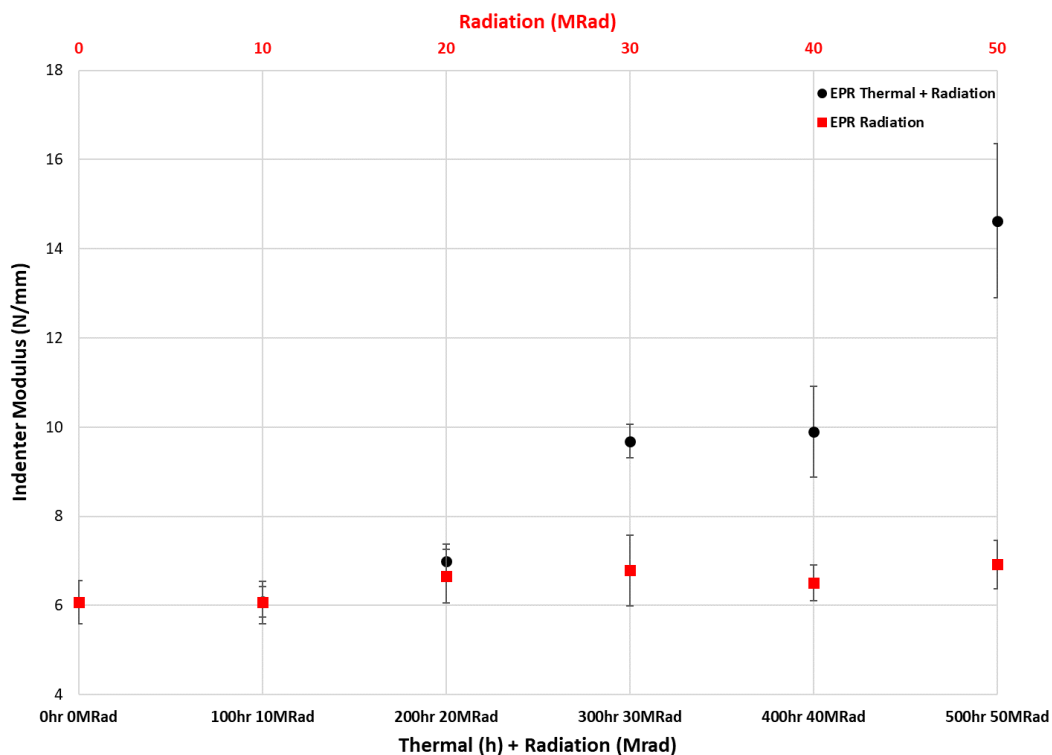


Figure 21. Indenter Modulus of EPR samples for the radiation only group (red) and the combined radiation thermal group (black)

5.3.3 OITP

Oxidation-Induction Temperature (OITP) testing was performed by Kinectrics staff and measured for the XLPE insulation by heating up small samples, approximately 5 mg, from room temperature to 300 °C at 10 °C/min in pure oxygen. The heat flow from the sample relative to a reference was recorded and the OITP reported as the onset of the oxidation of the sample, characterized by an exothermic peak. The results for the XLPE samples subjected to radiation-only, and radiation plus thermal, are provided in **Figure 22**. A clear decreasing trend was observed for the XLPE which experienced thermal and radiation aging, while no clear trend was measured for the radiation-only samples.

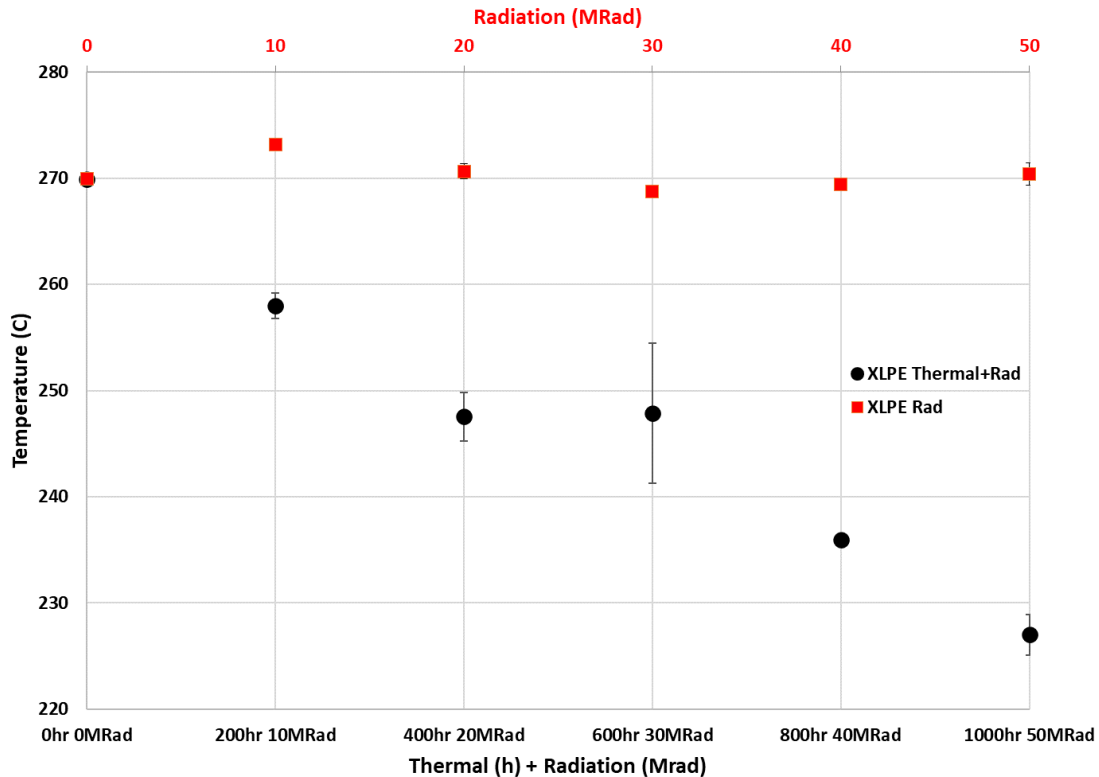


Figure 22. OITP of XLPE for the radiation only group (red) and the combined radiation thermal group (black).

6.0 DOSE TRACEABILITY AND MEASUREMENT UNCERTAINTY

Traceability to the NIST standard for the calibration of the Sunna film strip dosimeters is established through use of the measurement and test equipment (M&TE) listed in **Table 5**. The main M&TE included the ionization chamber used to calibrate the Co-60 field, the Co-60 field used to irradiate the Sunna film dosimeters and generate the calibration curve, the calibrated Sunna film dosimeters, and the fluorimeter used to read out the irradiated dosimeters.

The main error components used to calculate (via Root-Sum-of-the-Squares) the total measurement uncertainty associated with the measured dose rates and accumulated doses are listed in **Table 6**. The final value obtained was 6.6% at the 95% confidence level.

Table 5. M&TE Used in Support of Sunna Film Dosimetry Calibration.

| Standard / Item | Barcode [Identification No] | Calibration Expiration Date |
|---|------------------------------------|-----------------------------|
| Radiological Reference Standard | | |
| Exradin A12 Ion Chamber | ICSM1-0002 [XA151686] ^a | 11/2023 |
| Co-60 gamma-ray Field | 318-548/Top Port | 04/2024 |
| Non-Radiological Measuring and Test Equipment | | |
| Keithley 617 Electrometer | ECKE3-0002 [WA83570] | 10/2023 |
| Temperature/Pressure | WSCG1-0004 [N/A] | 03/2024 |
| Bertan Power Supply | N/A ^b | N/A ^b |
| Model TD700 Fluorimeter | s/n 7-1019-CE | 03/2024 |
| a. With Buildup Cap b. Accuracy of bias voltage supplied to the ionization chambers is not critical to the accurate response of the chambers. As such, there is not a requirement for traceable calibration of the power supply. | | |

Table 6. Main Error Components Used to Calculate the Total Uncertainty in the Measured Dose Rate and Accumulated Doses.

| Error Description | How Obtained? Estimated Distribution? | Pre-RSS Error Estimate (%) | |
|---|---|----------------------------|--------|
| | | Type A | Type B |
| Co-60 source field Air Kerma Rate calibration, Free-in-Air | RSS of all error components | N/A | 1.1 |
| Standard deviation of film readings for calibration set | SDOM | 1.0 | N/A |
| Drift of TD700 response (light source and PMT) during readout, as monitored by solid fluorescence standard | 1% max, assume rectangular distribution, so divide by SQRT (3) for 1 sigma. Drift was corrected based on solid std readings. | N/A | 0.6 |
| Positioning of Sunna film at desired source distance | 3% max, assume rectangular distribution, so divide by SQRT (3) for 1 sigma | N/A | 1.7 |
| Fit of regression curve to Sunna film data | 2% max, assume rectangular distribution, so divide by SQRT (3) for 1 sigma | N/A | 1.1 |
| Standard deviation of films irradiated in Mandrel stack | SDOM | 1.0 | N/A |
| Drift of TD700 response (light source and PMT) during readout, as monitored by solid fluorescence standard | 1% max, assume rectangular distribution, so divide by SQRT (3) for 1 sigma. Drift was corrected based on solid std readings. | N/A | 0.6 |
| Impact of irradiation temperature on film response | 0.5% max, assume rectangular distribution, so divide by SQRT (3) for 1 sigma | N/A | 0.3 |
| Impact of light effects on Sunna film | 0.5% max, assume rectangular distribution, so divide by SQRT (3) for 1 sigma | N/A | 0.3 |
| Impact of post-irradiation stabilization of film | 1% max, assume rectangular distribution, so divide by SQRT (3) for 1 sigma | N/A | 0.6 |
| Impact of nonuniformity of LiF loading along length of film roll | Measured SDOM of 2.5% for Roll A, but much of this spread is captured in the SDEV of the readouts for calibration set and unknowns. | 1.5 | N/A |
| Square Root of Sum of the Squares (RSS) Multiplied by coverage factor (k = 2) to obtain the Total Expanded Uncertainty at the 95% confidence level: 6.6% | | | |

7.0 CONCLUSIONS

Condition monitoring of electrical cables used in NPPs through electrical diagnostic techniques such as low frequency dielectric spectroscopy (LFDS) and time domain dielectric spectroscopy (TDS) or polarization depolarization current techniques (PDC), along with other reflectometry techniques such as frequency domain reflectometry (FDR) and time domain reflectometry (TDR) are of interest to the industry. However, very little research has been performed to evaluate these techniques for gamma-irradiated cable specimens. In this research work, PNNL performed gamma irradiation on mandrels of XLPE and EPR insulated cable provided by Kinectrics at the 318 HEF facility in Richland, WA. Doses in 10 Mrad (100 kGy) intervals, accurate to within ~6.6% (total uncertainty at the 95% confidence level) were delivered to 12 mandrels over ~104 days of irradiation (a total period of 7 calendar months due to pauses), with the highest dosed mandrels receiving ~70 Mrad (~700 kGy). Kinectrics performed the LFDS, TDS, TDR, and FDR measurements on these cables for most of the 10 Mrad (100 kGy) intervals to study the correlation of electrical and mechanical properties to radiation dose level.

With regards to the gamma-ray irradiation portion of the project, it was confirmed that, with a Co-60 source of sufficiently high activity, a passive dosimetry system of sufficient dose range, and the appropriate protocols, uniform doses varying from 10 - 60 Mrads (100-600 kGy) (~420 Mrad (~4200 kGy) total for all mandrels) can be delivered to 12 cable mandrels (~300' of total cabling) within approximately 100 days.

With regards to the results of post-irradiation testing of the cables, the electrical diagnostic and material testing showed the following effects or trends:

- For both 'single conductor' and 30' multiconductor 'mandrel' tests, different trends in the dielectric spectroscopy response were noted between the two aging regimes (thermal + radiation versus radiation only).
- Dielectric spectroscopy data showed trends of increasing tan delta at frequencies above 0.1 Hz across the 'single conductor' samples and 30' multiconductor 'mandrels'. A larger increase of tan delta is noted for samples subjected to progressive thermal + radiation aging than for exclusively radiation aging. Additional analysis metrics and condition indicators, especially for the more complex responses observed with the cable mandrels, will require more in-depth analysis of the data.
- Although both aging regimes (thermal + radiation and radiation only) created a decrease in elongation-at-break values at each subsequent aging interval, the combined thermal and radiation created a stronger decrease for both XLPE and EPR samples.
- The indenter results for EPR show that radiation aging did not create a trend in insulation hardness, whereas an increasing trend is clear for samples subjected to progressive thermal aging.
- A clear decreasing trend was observed for the OITP tests on XLPE which experienced thermal and radiation aging, while no clear trend was measured for the radiation-only samples.

The results of this study enable the extension or expansion of electrical assessment techniques for NPP electrical cables – providing operators more complete information to support repair, mitigation, or replacement decisions.

8.0 REFERENCES

- EPRI. 2017. Long-Term Operations: Initial Findings on Use of Dielectric Spectroscopy for Condition Monitoring of Low Voltage Nuclear Power Plant Cables. EPRI, Palo Alto, CA: 2017.3002010403.
- EPRI. 2022. Dielectric Spectroscopy of Low Voltage Nuclear Power Plant PVC Insulated Cables from EDF. EPRI, Palo Alto, CA: 2022. 3002023733.
- Gazdzinski, RF; Denny, WM; Toman, GJ; Butwin, RT. 1996. SAND96-0344 Aging Management Guideline For Commercial Nuclear Power Plants - Electrical Cable and Terminations
- Glass, SW; Jones, AM; Fifield, LS; Hartman, TS. 2016. Distributed Electrical Cable Non-Destructive Examination Methods for Nuclear Power Plant Cable Aging Management Programs. Pacific Northwest National Laboratory, Richland, WA
- Glass, SW; Jones, AM; Fifield, LS; Hartman, TS; Bowler, N. 2017. Physics-Based Modeling of Cable Insulation Conditions for Frequency Domain Reflectometry (FDR). PNNL-26493, Pacific Northwest National Laboratory, Richland, Washington
- IAEA. 2012. Assessing and Managing Cable Ageing in Nuclear Power Plants. International Atomic Energy Agency (IAEA), Vienna
- Joskow, P.L. 2006. The Future of Nuclear Power in the United States: Economic and Regulatory Challenges
- Murphy, MK; Kovács, A; Miller, SD; McLaughlin, WL. *Dose Response and Post-Irradiation Characteristics of the Sunna 535-nm Photo-Fluorescent Film Dosimeter*. Radiat. Phys. Chem., Vol 68, Issue 6, 2003, Pages 981-994, ISSN 0969-806X, [https://doi.org/10.1016/S0969-806X\(03\)00443-2](https://doi.org/10.1016/S0969-806X(03)00443-2).
- Murphy, MK; Kovács, A; McLaughlin, WL; Miller, SD; Puhl, JL. Sunna 535-nm photo-fluorescent film dosimeter response to different environmental conditions, Radiation Physics and Chemistry, Volume 68, Issue 6, 2003, Pages 995-1003, ISSN 0969-806X, [https://doi.org/10.1016/S0969-806X\(03\)00443-2](https://doi.org/10.1016/S0969-806X(03)00443-2).
- Suraci, SV; Fabiani, D; Xu, A; Roland, S; Colin, X. "Aging Assessment of XLPE LV Cables for Nuclear Applications Through Physico-Chemical and Electrical Measurements," in IEEE Access, 2020
- Suraci, SV; Fabiani, D; Colin, X; Roland, S. "Chemical and electrical characterization of XLPE cables exposed to radio-thermal aging," 2020 IEEE 3rd International Conference on Dielectrics (ICD)
- Twardoski B, Feldmann H, Bloom ME, Ward J. Modern dosimetric tools for (60)Co irradiation at high containment laboratories. Int J Radiat Biol. 2011 Oct;87(10):1039-44. doi: 10.3109/09553002.2011.598210. PMID: 21961968; PMCID: PMC3196598.
- Verardi L, Fabiani D, Montanari GC, Gedde UW, Linde E. "Aging investigation of low-voltage cable insulation used in nuclear power plants," in 2012 Annual Report Conference on Electrical Insulation and Dielectric Phenomena, 2012, pp. 851–854.

Pacific Northwest National Laboratory

902 Battelle Boulevard
P.O. Box 999
Richland, WA 99354
1-888-375-PNNL (7665)

www.pnnl.gov